Ductility of Precast Prestressed Piles

Andrew Budek, PE PhD, Department of Civil Engineering, Texas Tech University, Lubbock, TX 79409-1023
Gianmario Benzoni, PhD, Department of Structural Engineering, University of California at San Diego, La Jolla, CA 92093-0085

Abstract

A parametric study of the inelastic seismic response of precast prestressed piles was undertaken to predict the ductility available from these structural elements. The work was done using a nonlinear inelastic finite-element program written specifically for this project, and validated through both laboratory and in-situ testing. The study examined single piles using several types of pile-cap connection, and the effect of the addition of mild steel reinforcement, under varying levels of avail load, and for a range of soil stiffness. The results indicated that precast prestressed piles are structural elements of limited ductility. Assuming that the pile-cap connection is detailed to allow and support the formation of a plastic hinge at the pile-cap connection, with subsequent redistribution of moment down the shaft to form a secondary subgrade hinge in the pile shaft, the maximum suggested displacement ductility for design is 2.5. The addition of mild steel longitudinal reinforcement was not found to enhance ductility (though it may be needed to develop the required flexural strength). The optimum pile-cap connection to maximize ductility is embedment of the pile head into the cap. Rotation capacity is maximized by embedment of the prestressing tendons (and any mild steel longitudinal reinforcement present) into the pile cap.

Keywords: Footings, Piles, Precast, Prestressed, Seismic, Soil-structure

Background and Scope of Work

The use of prestressed concrete piles as foundation elements was first developed in the early 1950's. They offer a number of advantages to the designer and contractor. Inherently resistant to tensile stresses, they can be economically fabricated at a convenient location, safely transported, and handled during the driving process. The ability to take tensile stress without cracking is very advantageous in that inadvertent tensile stresses applied during construction or service will be less likely to lead to cracking, thus reducing the risk of corrosion.

Piles carry both axial load and lateral force. Axial load is resisted by a combination of end bearing and skin friction (the dominant mechanism being determined by the soil characteristics). Lateral force, imposed, for instance, by seismic excitation of the superstructure, is resisted by a combination of shear and bending resistance (it is interesting to note that early pile design assumed that axial loads only could be carried, and until relatively recently pile lateral strength was rarely checked).

While, ideally, a foundation would be designed to remain elastic under seismic attack (as repair of damage to piles after an earthquake is at best difficult), this is not normally practical for pile/column designs, and hinging of piles in pilecap configuration may be difficult to avoid. Thus, the inelastic behavior of prestressed piles warrants study. Under lateral loads imposed by an earthquake, an individual pile (with a fixed head condition) may be expected to develop a moment pattern of the shape shown in Fig. 1.

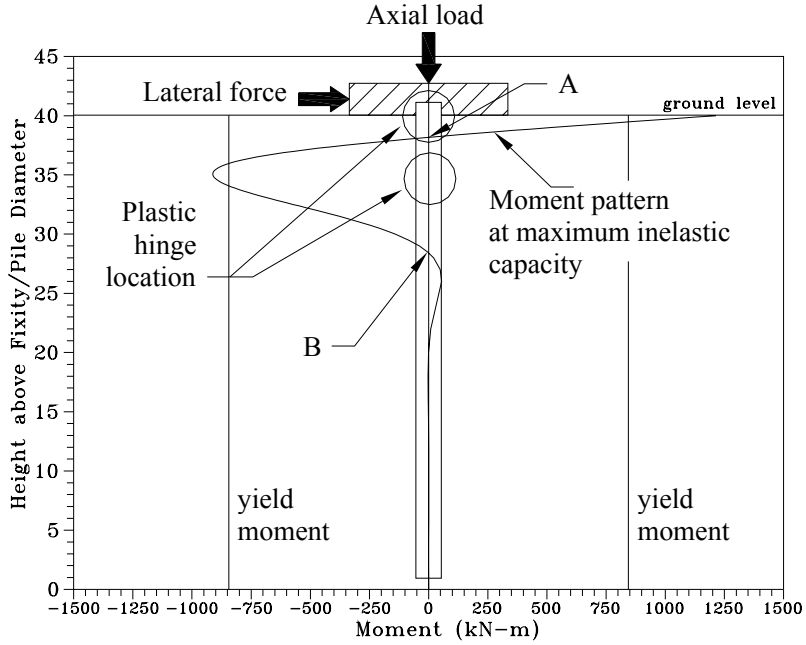

Fig. 1: Pile moment pattern resulting from axial and lateral load

Inadequate detailing of early prestressed piles may have caused inadequate performance in several earthquakes, such as the 1964 Alaskan[1] and 1972 Miyagi-Ken-Oki[2] events. The relation of detailing deficiency to poor performance has been identified by several researchers[3,4,5].

Beyond proper detailing, however, a systematic investigation of the inelastic response of prestressed piles to lateral loading is needed, modeling the full soil-structure system using nonlinear inelastic constitutive models.

Finite-element analysis for soil-pile interaction has been verified through field studies in the past[6]. It is a very powerful tool, as it allows great flexibility in representing both pile and soil properties.

The subject of the present research is therefore to perform a parametric study on the nonlinear inelastic lateral response of piles to seismic loading, characterizing the behavior of the soil-pile system using varying axial load, soil stiffness, and pile-cap connection details. The objective is to generate recommendations for ductile pile performance that can be used in assessment and design.

Analytical Modeling

The analytical models of the soil-pile system used in this work were based on the nonlinear inelastic finite-element modeling of a Winkler beam (a beam on a flexible foundation). The pile was represented using beam elements, and the soil using lateral springs acting at the nodes (Fig. 2).

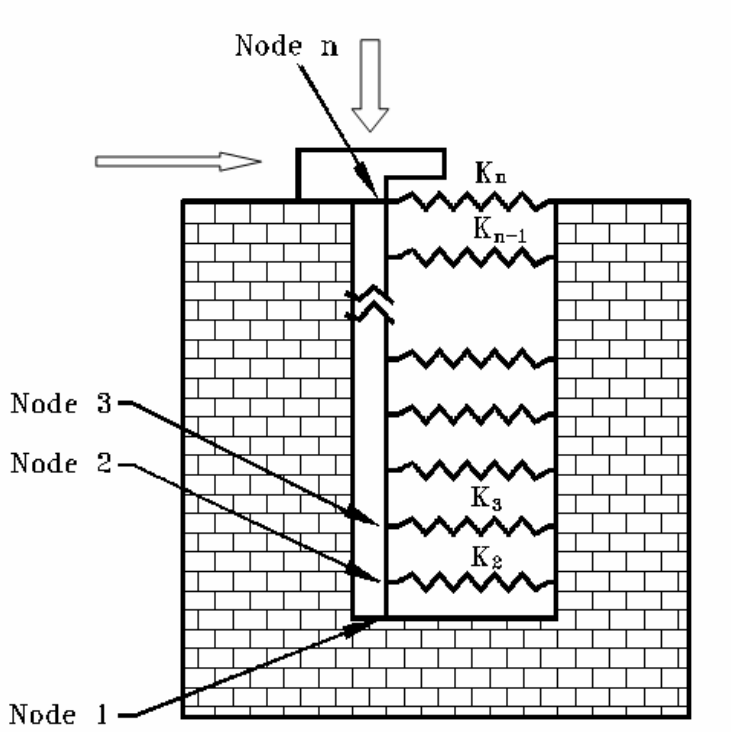

Fig. 2: Prestressed pile analytical model with indicated forces (the notch in the cap of the prestressed model is for illustrative purposes, to allow the top spring to be shown)

Nonlinear inelastic constitutive models were used for both the pile and soil, and have been described in detail elsewhere[9]. Briefly, the change in flexural stiffness of the pile as inelastic action took place was extracted from the moment-curvature data, as the slope of the moment-curvature curve. Lateral load was applied in a series of steps. Elements' flexural

stiffnesses were modified as necessary after each load step, according to the elements' respective average moment. Pile yield was defined by tendon stress reaching 85% of its ultimate value.

A bilinear soil model was used, in which the lateral stiffness of the soil (i.e., individual spring stiffness) was reduced to one-fourth of its original value when the displacement at a node associated with a given spring exceeded 25.4 mm.

Soil stiffness, as expressed by the subgrade reaction modulus K, ranged from 3200 to 48000 kN/m^3. Where it is treated as an independent parameter used to describe the behavior of a specific variable (such as displacement ductility as a function of soil stiffness) it is included in a derived quantity, the nondimensional system stiffness (KD^6/D^*EI_{eff}), which includes cracked-section flexural stiffness (EI_{eff}) of the pile shaft, and in which the pile diameter D is normalized against a 'reference' pile (D^*=1.83 m) described in previous work[9]. The validation of this approach against experimental results is described below.

In the present work, the structure was modeled as a continuous pile of diameter D=0.61 m. Depth to the pile base was set at 24.38 m (40D), which exceeds that corresponding to 'long-pile' response. The pile head was assumed to connect to a cap at ground level. Axial load was varied from zero to $0.4f'_cA_g$, to represent forces from global overturning moments transferred from the superstructure. The pile section used in the analysis was a typical 0.61 m diameter round pile as used in California; details are shown in Fig. 3. Nominal effective section prestress (after losses) is 9.3 MPa.

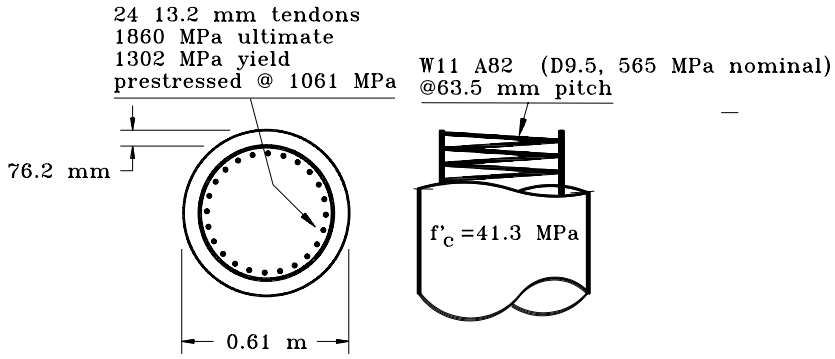

Fig. 3: Prestressed pile section

Three different types of pile-pile cap connection were considered; each was examined with and without the presence of mild steel longitudinal bars providing dowel reinforcement through the pile-cap connection, and down through the area of the subgrade plastic hinge (Fig. 4). The piles' flexural response was analyzed using the Mander[13] model for confined concrete modified for prestressed sections. Modifications allowed for appropriate positioning of tendons, with the correct level of prestressing force.

Modeling of the different connections was addressed through variation of either section prestress or axial load in calculating moment-curvature data. For the pile head embedded in the cap, full prestress was assumed at the bottom of the cap (i.e., full transfer was assumed at the interface) (Fig. 4). To model embedment of the tendons, effective prestress was assumed to go from zero at the top of the pile to its full value at the end of the transfer length of 115 d_b. This part of the pile was therefore modeled in ten sections, adding 10% of the effective prestress each time. The input data for this case therefore consisted of eleven sets of moment-curvature data

(output from the Mander model analysis), applied to the relevant section of the pile. The practice of stressing the tendons through the pile cap was handled similarly; active prestress went from zero to its full value over the transfer length, and the effect of stressing the tendons was modeled by applying an axial load to each section, such that the combination of axial and prestress load would remain constant (i.e., 40% of prestress at 40% of d_b was supplemented by 60% of axial load from stressing through the cap).

Strain penetration into the cap is an important part of modeling; in the response of actual structures it permits a somewhat larger rotation at the pile-cap connection. It was modeled in the present work by decreasing the stiffness of the pile's top element as yielding of the tensile reinforcement occurred, and is described in more detail below.

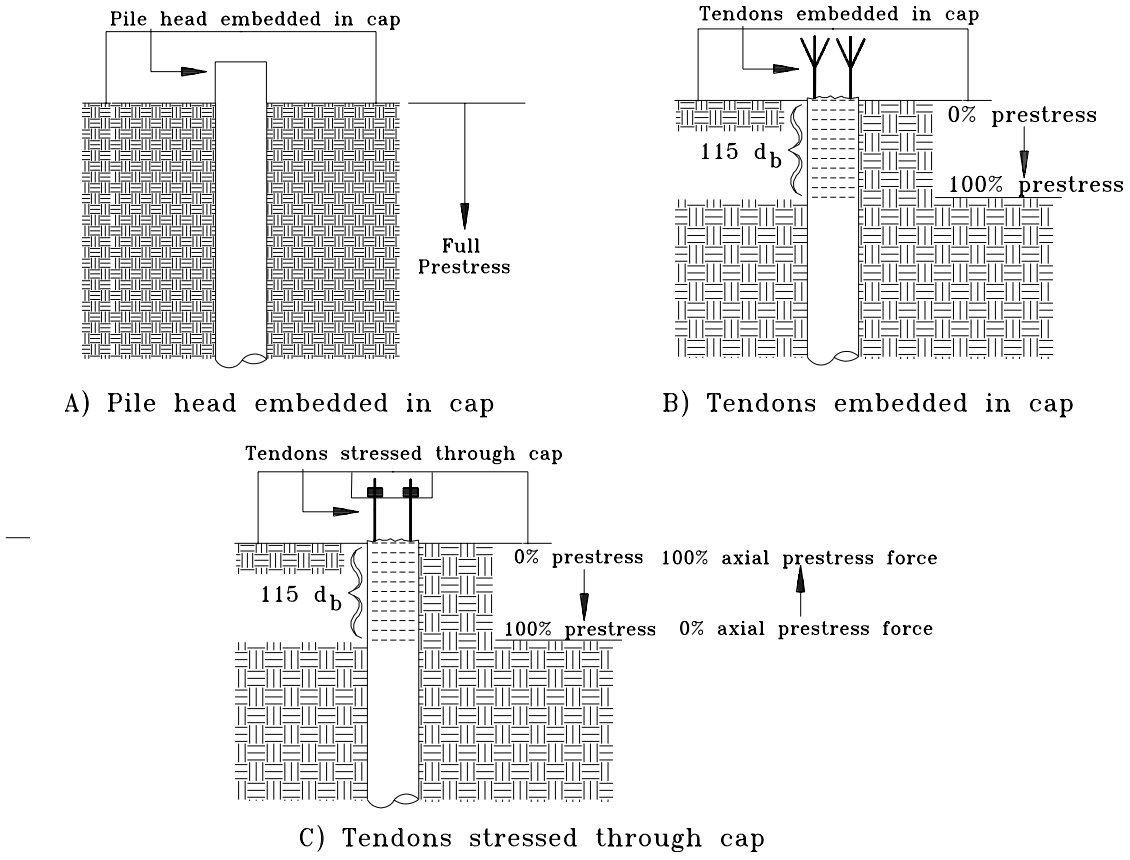

Fig. 4: Prestressed pile-pile cap connections considered in this study (shown without reinforcing steel dowels). Nominal embedment length of (A) is two pile diameters D.

The FEA program used was written specifically for this research program and was validated through comparison with laboratory testing[7,8,9,10,11], and against results from in-situ testing[12].

The laboratory testing program consisted of a series of sixteen tests, which included a number of precast prestressed pile shafts of a size and configuration similar to those examined in the current work[8]. The purpose of the investigation was to characterize the effect of external confinement (as may be provided by competent soil) on the flexural ductility available in the pile shaft at the subgrade hinge (between points "A" and "B" in Fig. 1). The finite element model

used in the current work was utilized to predict pile shaft response under the imposed loading, and was successful.

The analytical model was further validated by comparison with a series of four in-situ tests of free-head reinforced concrete pile-columns performed by Chai and Hutchinson[12]. In these tests, 0.406 m diameter piles were embedded in soil placed under controlled conditions into a purpose-built soil box, and tested under combined axial and lateral load. The force-displacement envelope, and predicted response, from the first of these tests is shown in Fig. 5.

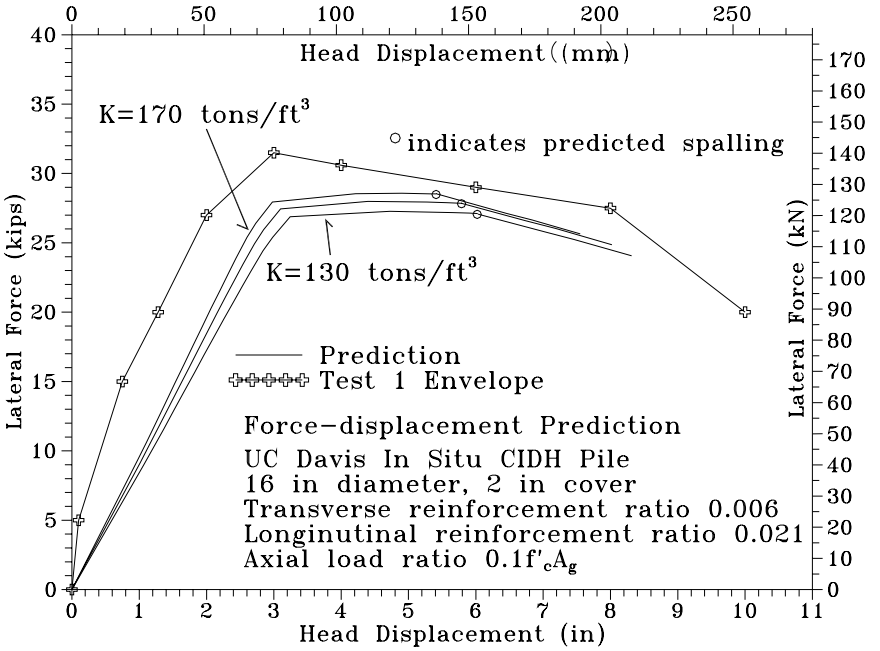

Fig. 5 – Comparison of finite-element model prediction with in-situ pile test[12]

It is clear that the general trends of the test results, such as elastic stiffness, beginning of the softening branch, and incipient failure are faithfully reproduced by the prediction. There are some discrepancies, which may be attributed to conservative modeling assumptions. First, the initial stiffness of the test pile was higher than the prediction. This comes from the action of the small-strain modulus of elasticity of the soil, which is estimated at four times the large-strain value[13] (Bowles). This 'factor of four' difference is quite close to that shown in Fig. 2. Second, the maximum lateral force was underpredicted by the model, by about 12%. This can be directly attributed to the use of the 28-day concrete strength to generate the prediction, rather than day-of-test strength. This was the prediction placed on the plotter at the test site, and it should therefore remain.

Use of the nondimensional system stiffness term KD^6/D^*EI_{eff} was also validated through comparison with this is situ testing program. One observation from previous analytical work was that the center of the plastic hinge in the pile shaft (i.e., the subgrade hinge) would move toward the surface as plasticity progressed, from the original location of the point of maximum subgrade moment. Its terminal location when the ultimate inelastic capacity of a free-head pile (in which the subgrade hinge controls response) can therefore be predicted; it is consistently at a depth 70% of that of the point of maximum subgrade elastic moment, a value which is insensitive to either soil stiffness or abovegrade height of the pile head (the actual depth is of course a function of both of these variables).

In Fig. 6 are shown curves predicting subgrade hinge depths for the abovegrade heights tested, in the relevant range of nondimensional system stiffness. The depths of the centers of the plastic hinges, determined by digging down to the center of the plastic region after testing, fall almost directly on the curves.

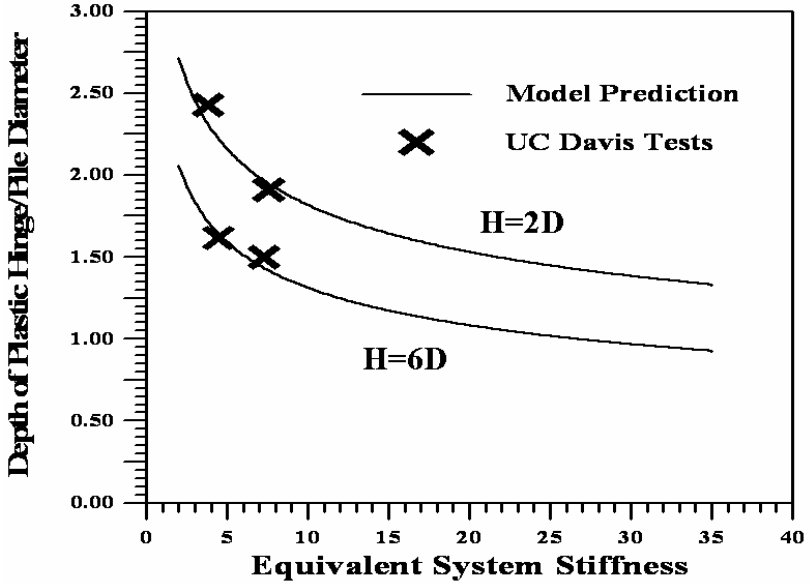

Fig. 6: Comparison of predicted and observed plastic hinge depth from in-situ pile tests[12]

For plastic hinges forming against supporting members such as footings or cap beams, theoretical and experimental studies have led to the development of the following equation for plastic hinge length[14]

$$l_p = 0.08L + 0.022f_y d_{bl} \qquad (1)$$

where L is the distance from the critical section to the point of contraflexure, f_y is the yield strength in MPa, and d_{bl} is the longitudinal bar diameter. The first term in equation 1 represents the spread of plasticity resulting from variation in curvature with distance from the critical section, and assumes a linear variation in moment with distance. The second term represents the increase in effective plastic hinge length associated with strain penetration into the supporting member.

Figure 1.8 shows that equation 1 somewhat overestimates the plastic hinge length for the hinge occurring at the pile-pile cap connection. Using typical values from an elastic analysis for depth to point of contraflexure at yield for a pile with the pile head embedded into the cap (both with and without reinforcing dowels), the plastic hinge length is seen to be substantially greater than that resulting from the present inelastic analysis. Used in this context, equation 1 falls victim to one of the pitfalls of elastic analyses of piles [9]; when yielding is reached in the pile's critical section, the structure softens, and a lesser depth of soil needs be mobilized, thus moving the point of contraflexure toward the surface. If an appropriate correction is made, equation 1 gives a reasonably good prediction of l_p. (The second term in eqn. 1, representing strain penetration, is straightforward in cases in which dowels are present, as the dowels' yielding is concurrent with the yield point of the structure. Where prestressing tendons alone form the

longitudinal steel, however, interpretation is complicated by the fact that tendons in general require a considerably greater development length than does deformed nonprestressed reinforcing steel. Also, ultimate tensile strains in prestressing steel are considerably lower than in ordinary reinforcing steel, and even this is compromised by proximity to anchorages, with their attendant stress risers. Accordingly, in this study the strain penetration length for prestressing tendons was assumed to be roughly equivalent to that resulting from the use of Grade 60 #9 deformed bar (D28.6, 455 MPa nominal yield).)

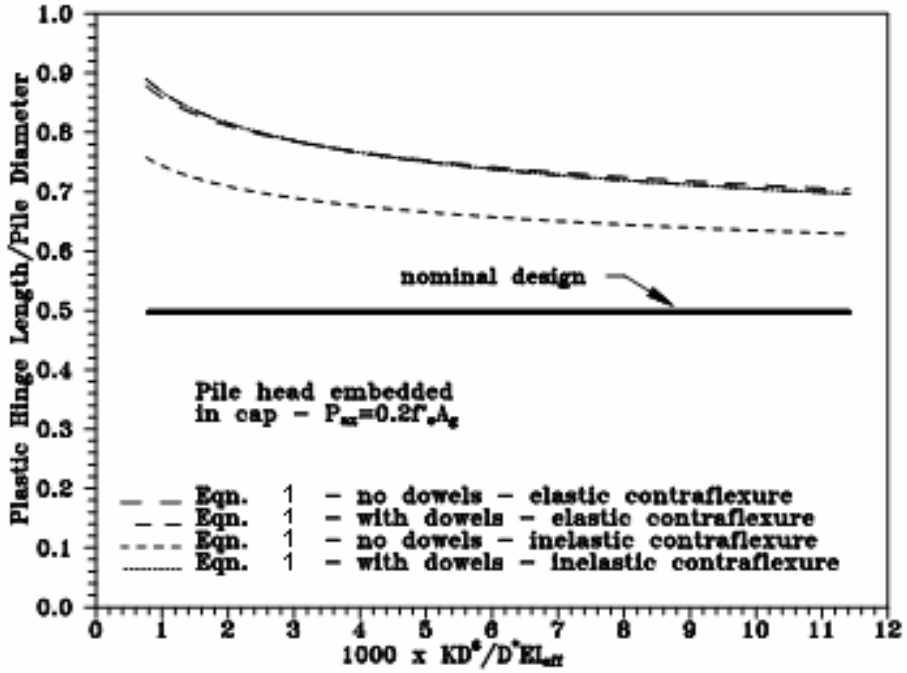

Fig. 1.8: Calculated plastic hinge lengths - comparison of equation 1 with nominal design value (prestressed pile with head embedded in cap - no nonprestressed longitudinal reinforcement)

It is apparent that eqn. 1 is inappropriate for plastic hinges forming in pile shafts since (a) inelastic curvature can be expected to spread both above and below the critical section, (b) the slope of the moment profile at the section of maximum moment is zero, invalidating the assumption of a linear decrease in moment with distance from the critical section, and (c) there should be no strain-penetration effect, since at the critical section there should be no significant slip of tension reinforcement past the section (which results in the strain penetration effect for a fixed-base plastic hinge) because of the approximate symmetry of the moment profile about the critical section.

Results

Flexural Response and Moment Patterns

The response of piles to lateral loading is best introduced through examination of moment patterns. In the case of a fixed-head pile, the maximum moment (which controls overall response) will be generated at the pile-cap connection, and a secondary moment maximum forms

below grade. Modeling inelastic pile response results in the formation of a plastic hinge at the pile-cap connection, after which moment is redistributed into the shaft. This may result in the formation of a secondary hinge in the shaft. This is demonstrated in Figs. 5 – 7, in which the effect of varying soil stiffness and axial load on pile response is represented for the case of the pile head embedded into the cap (analysis of other end conditions, and considering the presence of dowels, show similar trends). Ultimate moment vs. height for three levels of axial load, P_{axial}=0, $0.2f'_cA_g$, and $0.4f'_cA_g$, and yield moment for the pile shafts is represented. Increasing soil stiffness increases the maximum magnitude of the subgrade moment. Stiffening soil reduces the shear span between the two moment maxima, which requires greater mobilization of the pile shaft flexural capacity at the subgrade moment maximum. Also, lower axial load (with a commensurate reduction of section flexural strength) places more demand on the pile shaft to assist in resisting the applied moment.

The effect of moment redistribution can only be assessed through an inelastic analysis. An important aspect of this is shown in Figs. 8 and 9. Fig. 8 compares an inelastic analysis with an elastic analysis of the system to maximum flexural strength. While the ultimate moments at the pile head are similar, the secondary maxima in the pile shaft differ markedly, in that the shaft maximum predicted by elastic analysis is much lower. The consequence of this is seen in Fig. 9, which shows the difference in shear predictions from inelastic and elastic analyses. The redistribution of moment down the pile shaft after formation of the hinge at the pile-cap connection creates much higher levels of shear (approaching twice as much, in the worst cases) in the pile shaft, which is missed by a purely elastic analysis. The increase in shear is also caused by the point of maximum moment in the shaft moving upward, toward ground level, as the subgrade hinge forms. This effect reduces the shear span, and has been previously observed in both analytical[9] and experimental[12] work.

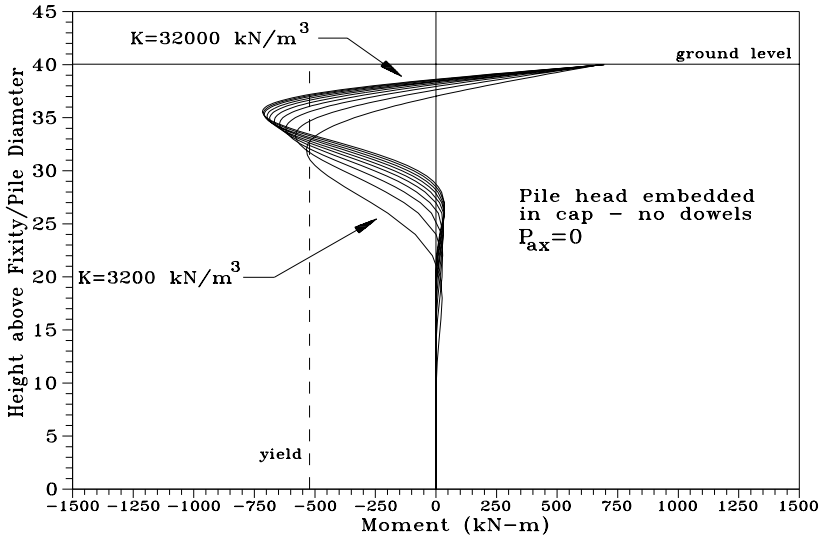

Fig. 5: Moment vs. height, P_{axial}=0, pile head embedded in cap, no reinforcing dowels

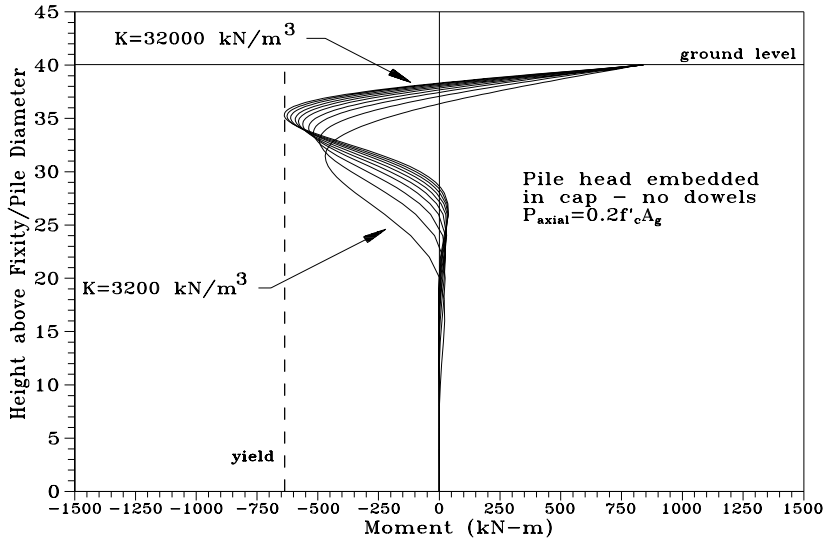

Fig. 6: Moment vs. height, $P_{axial}=0.2f'_cA_g$, pile head embedded in cap, no reinforcing dowels

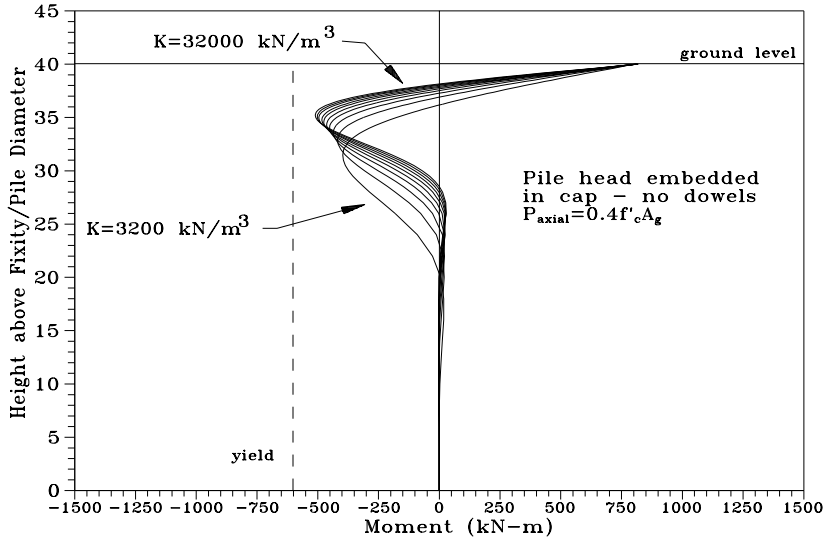

Fig. 7: Moment vs. height, $P_{axial}=0.4f'_cA_g$, pile head embedded in cap, no reinforcing dowels

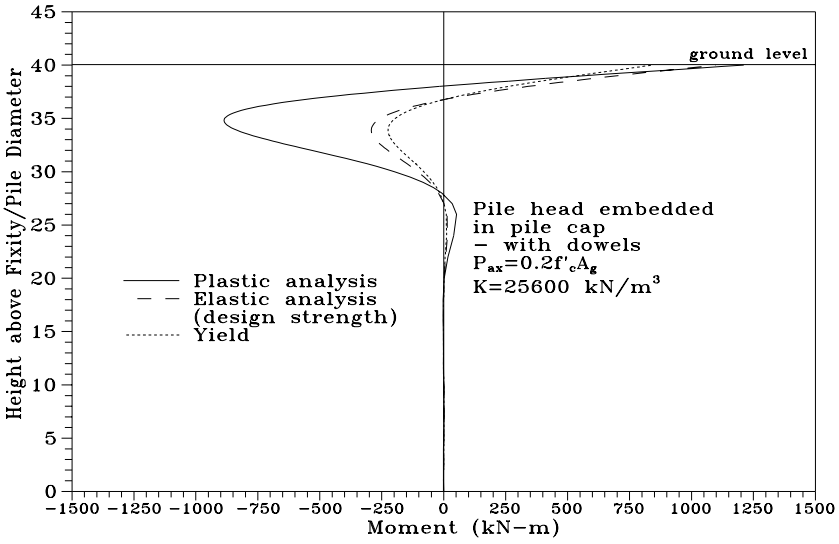

Fig. 8: Moment vs. height, comparison of inelastic and elastic analyses, $P_{axial}=0.2f'_cA_g$, pile head embedded in cap, with mild steel reinforcing dowels

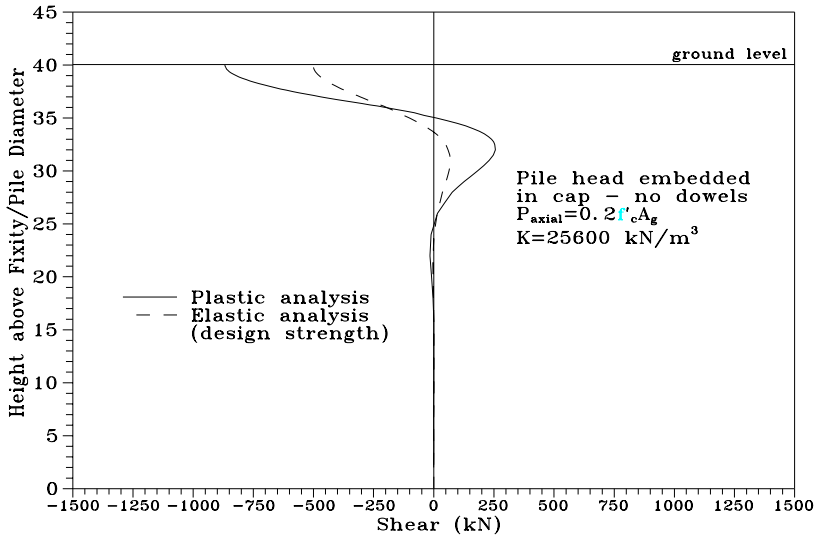

Fig. 9: Shear vs. height, comparison of elastic and inelastic analyses, pile head embedded in cap (with mild steel reinforcing dowels), $P_{ax}=0.2f'_cA_g$

Figs. 10 and 11 show the depth of the point of maximum subgrade moment for piles without, and with, mild steel longitudinal reinforcement, respectively. This is an important parameter as it shows the length of pile for which detailing for inelastic flexural action should be provided, in the form of increased levels of transverse reinforcement.

Depth of the maximum subgrade moment (or hinge, if one forms) is strongly affected by system stiffness, but weakly by structural details such as the presence of mild steel reinforcement or the specific type of pile-cap connection evaluated. The maximum depth seems to approach a limiting value as system stiffness (functionally, in the case of the piles examined here, soil

stiffness) increases. The overall range is from 9 diameters, for very soft soils, to 4 diameters. The analysis was not extended for softer soils, on the assumption that 'pole' behavior (i.e., rotation of the pile as a whole) would begin to take place as stiffness was dropped to very low levels.

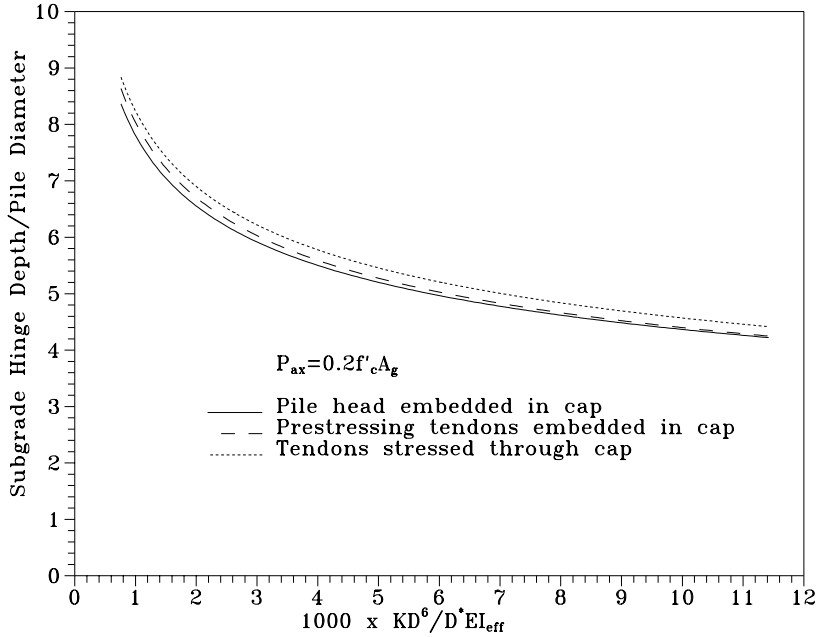

Fig. 10: Depth of maximum subgrade moment, comparison of different pile-pile cap connections, mild steel reinforcing dowels absent

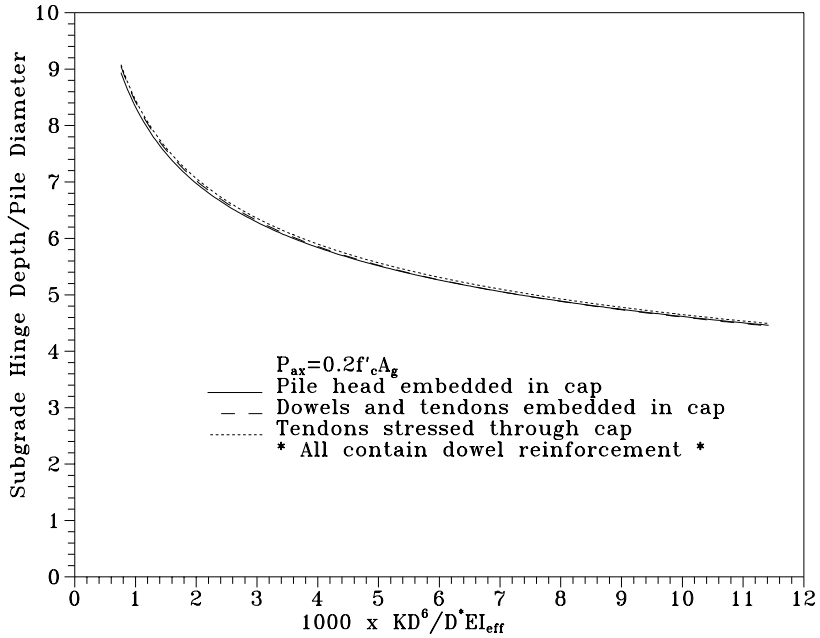

Fig. 11: Depth of maximum subgrade moment, comparison of different pile-pile cap connections, mild steel reinforcing dowels present

Comparison of Pile-Cap Connections

Fig. 12 compares ultimate moment patterns for the three pile-pile cap configurations examined (pile head embedded in cap, prestressing tendons embedded in cap, tendons stressed through cap) in which reinforcing dowels were not included. Fig. 13 examines the effect of the presence of mild steel longitudinal reinforcement on moment patterns for these configurations. Curves are shown for both soft and stiff soil, at a moderate axial load. The greatest demand on the pile shaft comes from embedding the tendons into the pile cap (Fig. 12). This comes from the reduced flexural strength of the 'embedded tendon' condition. In this case prestress is assumed to be developed over the transfer length of 115 d_b, beginning at ground level (Fig. 4). The effective prestress force at the connection is therefore zero, which gives a lower strength and flexural stiffness over the plastic hinge length of 0.5 D (D= pile diameter) at the pile-cap connection, requiring greater mobilization of the pile shaft. (The transfer length is about 2.2 pile diameters, so the active prestress over the hinge length of 0.5D does not exceed 30% of total prestress.)

The presence of reinforcing dowels in the three categories of pile-pile cap connection reduced the differences between subgrade moment maxima (Fig. 13). In both cases, the differences between subgrade moment maxima among the different end conditions are larger for softer soils.

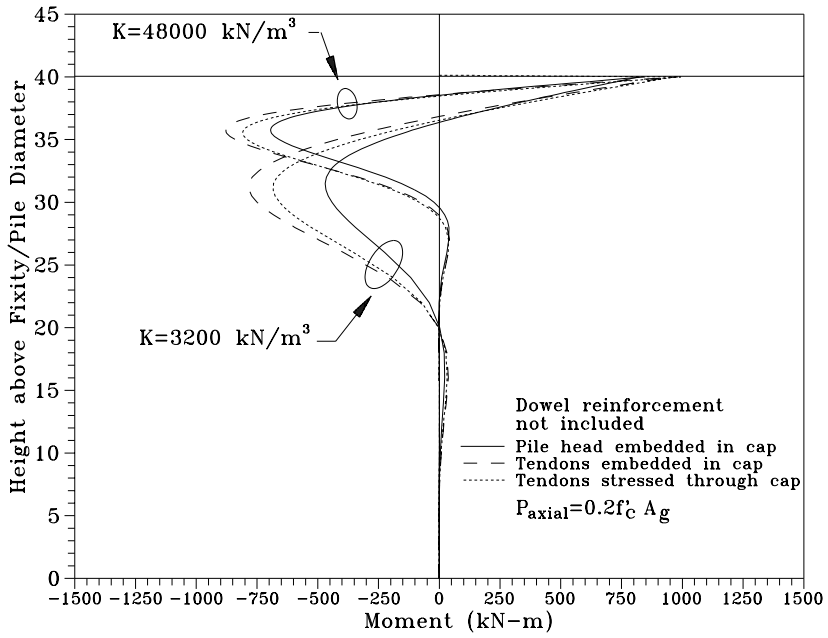

Fig. 12: Comparison of ultimate inelastic moment patterns for different pile-pile cap connections, reinforcing dowels absent, $P_{ax}=0.2f'_cA_g$

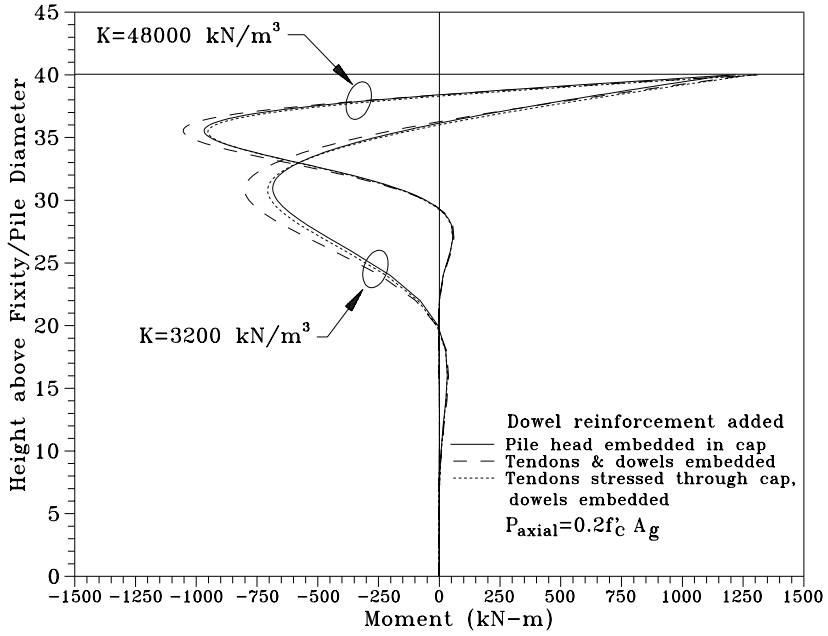

Fig. 12: Comparison of ultimate inelastic moment patterns for different pile-pile cap connections, mild steel reinforcing dowels present, $P_{ax}=0.2f'_cA_g$

System Ductilities

In Fig. 13 and 14, displacement ductility is shown as a function of nondimensional system stiffness, axial load, and pile-cap connection type. Fig. 13 shows displacement ductility capacity for piles without mild steel longitudinal reinforcement, and Fig. 14 shows displacement ductility capacity for piles with mild steel reinforcement.

A brief perusal of both Figures shows that displacement ductility capacity is relatively insensitive to the parameters studied. The plots lie on a fairly narrow range.

The most prominent general trends are an increase in ductility capacity with both axial load and soil stiffness (expressed here as nondimensional system stiffness). Inclusion of mild steel reinforcement has a significant effect. Comparing Figs 13 and 14 shows that such reinforcement both increases ductility at the lower end of its range, and decreases it at the top end of the range.

In both cases, embedding the pile head into the cap gives the largest displacement ductility capacity. For piles without mild steel reinforcement, the maximum range of ductility for this case is from 2.5 to 4; with reinforcement the range is about 2.7 to 3.4.

Embedding the tendons (and dowels, where present) gives the next-highest ductility, followed by the rarely-used practice of stressing the tendons through the footing.

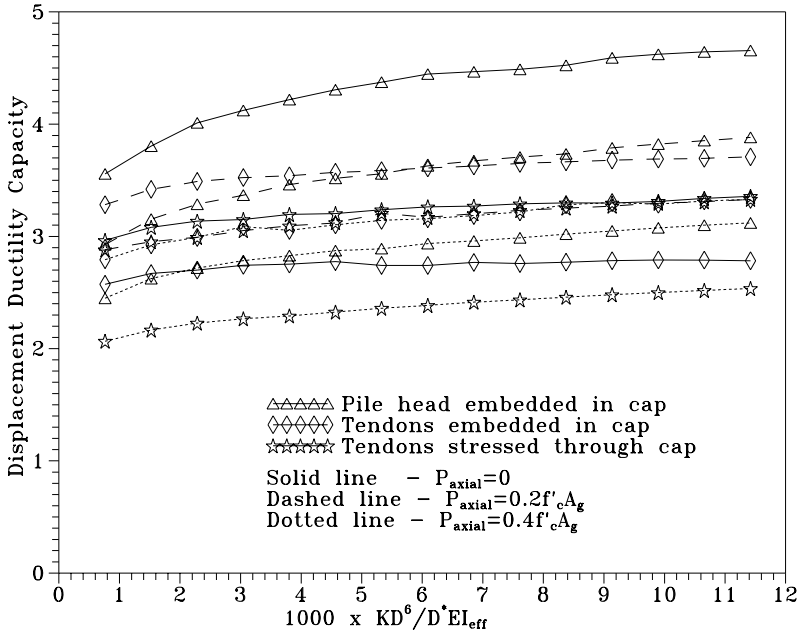

Fig. 14: Displacement ductility capacity vs. nondimensional system stiffness, comparison of piles without mild steel reinforcing dowels, $3200 \leq K \leq 48000$ kN/m^3

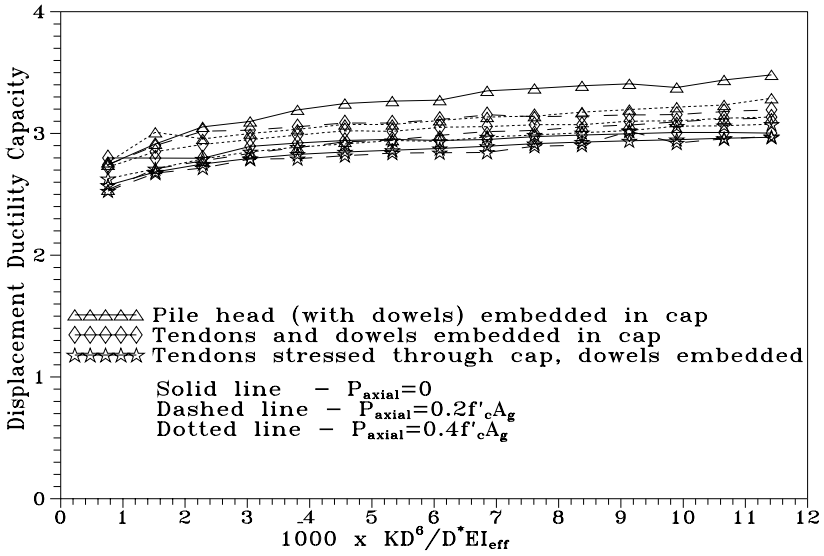

Fig. 15: Displacement ductility vs. system stiffness for piles with dowel connection to cap for varying axial load and connection details.

Depth to Fixity for an Equivalent Cantilever

The equivalent cantilever approach has been used for pile design for many years. Briefly, the soil-pile system is replaced by a fixed-base column which has the same displacement at yield as the pile.

In fig. 17

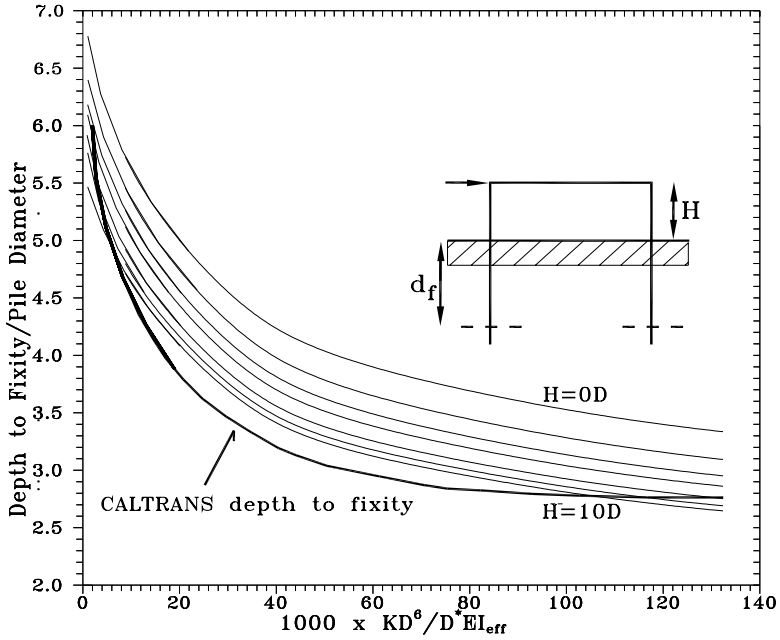

Conclusions

The results from this research program allow the formulation of several conclusions which may be used in design.

First, prestressed piles can be considered as ductile structural elements. This has been shown experimentally through previous research, and verified through the analytical work described above. The consequence of this is that, with appropriate detailing, prestressed piles may be used as energy-dissipating elements in structures in which ductile behavior may be demanded. Detailing that would allow sufficient ductility capacity can be specified in both reinforcement specification (through relevant design codes) and location (through knowledge of the location of the point of maximum subgrade moment).

Second, the ductility capacity of prestressed piles is limited, and is affected by both the connection type chosen, and axial load. The connection type is intrinsic to the structure of which the piles form a part, but axial load may be subject to variation in a given pile.

The following recommendations are therefore put forward:

- For the case of pile caps embedded in the cap to a depth at least equal to the tendon transfer length, displacement ductility should be set at a maximum of 2.5
- For all other cases that are applicable to the configurations examined in this research, a maximum ductility capacity of 2 should be used.
- Transverse reinforcement that would support formation of a plastic hinge (such as that called for by CALTRANS for columns[14]) should be provided to a depth of at least ten pile diameters below the cap.

References

1. Kachedoorian, R. (1968), “Effects of March 27, 1964 Earthquake on the Alaska Highway System”, U.S. Department of the Interior, U.S. Geological Survey Professional Paper 545-C, Washington, DC
2. Kishida, H., Hanazato, T., and Nakai, S. (1980), “Damage of Reinforced Precast Piles during the Miyagi-Ken-Oki Earthquake of June 12, 1972”, *Proceedings of the Seventh World Conference on Earthquake Engineering*, Istanbul, Turkey
3. Falconer, T.J., and Park, R. (1982), Ductility of Prestressed Concrete Piles under Seismic Loading, Research Report No. 82-6, Department of Civil Engineering, University of Canterbury, New Zealand
4. Sheppard, D.A. (1983), "Seismic Design of Prestressed Concrete Piling", *PCI Journal*, vol. 28, no. 2, pp. 20-49
5. Banerjee, S., Stanton, J.F., and Hawkins, N.M. (1987), "Seismic Performance of Precast Concrete Bridge Piles", *Journal of Structural Engineering, ASCE*, vol. 113, no. 2, pp. 381-396
6. Priestley, M.J.N. (1974), "Mangere Bridge Foundation Cylinder Load Tests", MWD Central Laboratories Report No. 488, 1974
7. Budek, A.M., Benzoni, G., and Priestley, M.J.N (1995), An Analytical Study of the Inelastic Seismic Response of Reinforced Concrete Pile Shafts in Cohesionless Soil, Department of Structural Engineering, University of California at San Diego, La Jolla, California, Report No. SSRP 95/13
8. Budek, A.M., Benzoni, G., and Priestley, M.J.N (1997), Experimental Investigation of Ductility of In-Ground Hinges in Solid and Hollow Prestressed Piles, Department of Structural Engineering, University of California at San Diego, La Jolla, California, Report No. SSRP 97/17
9. Budek, A.M., Priestley, M.J.N., and Benzoni, G. (2000), “Inelastic Seismic Response of Bridge Drilled-Shaft RC Pile/Columns” *Journal of Structural Engineering, ASCE*, vol. 126, no. 4, pp. 510-17
10. Budek, A.M., Priestley, M.J.N., and Benzoni, G. (2004), “The Effect of External Confinement on Flexural Hinging in Drilled Pile Shafts”, *Earthquake Spectra, EERI,* vol. 20, no. 1, pp. 1-20
11. Budek, A.M., Priestley, M.J.N. (2005), “Experimental Analysis of Flexural Hinging in Hollow Marine Prestressed Pile Shafts”, *Coastal Engineering Journal, JSCE,* vol. 47 no. 1, pp. 1-20
12. Chai, Y.H., and Hutchinson, T.C. (2002), “Flexural Strength and Ductility of Extended Pile-Shafts – Experimental Study”, *Journal of Structural Engineering, ASCE,* vol. 128, pp. 595-602
13. Mander, J.B., Priestley, M.J.N., and Park, R. (1988), “Observed Stress-Strain Behavior of Confined Concrete,” *Journal of Structural Engineering, ASCE,* vol. 114, pp. 1827-49
14. Priestley, M.J.N., Seible, F., and Calvi, G (1996), Seismic Design and Retrofit of Bridges, John Wiley and Sons, New York